ANEXOS

ANEXO I. IMPEDANCIA ESPECÍFICA PARA LAS MEDIDAS INVASIVAS NO TRANSMURALES Y TRANSMURALES EN LOS DIFERENTES ESTADOS DEL TEJIDO DE MIOCARDIO: SANO, ISQUEMIA Y CICATRIZ

En este anexo, se exponen los resultados de las medidas invasivas realizadas en animales (cerdos). Cada una de las tablas contiene la resistividad y fase del tejido de miocardio sano, isquemia aguda y cicatriz. Los valores se muestran para las 25 frecuencias medidas (1 kHz a 1 MHz).

Los resultados han sido agrupados por: el método de medida utilizado:

- No Transmural el parámetro de resistividad (Ω·cm) Tabla I-1 y fase (º) Tabla I-2 del grupo I (n = 7) tejido sano e isquemia aguda y grupo II (n = 7) para cicatriz.
- Transmural, el parámetro de resistividad (Ω·cm) Tabla I-3 y fase (º) Tabla I-4 del grupo III para el tejido sano (n = 9), isquemia aguda (6) y cicatriz (n = 17).

Los valores están expresados en valor medio y desviación estándar (SD).

Tabla I-1. *Resistividad* (Ω•cm). Medidas invasivas *No Transmurales* realizadas en animales (cerdos). Valores de los diferentes estados del tejido de miocardio sano, isquemia aguda y cicatriz.

	Sano		Isquemia Aguda		Cicatriz	
Frecuencia	Valor Medio	SD	Valor Medio	SD	Valor Medio	SD
1.00	254.00	51.57	554.94	120.28	122.00	26.35
1.33	253.54	50.80	536.19	108.16	125.90	27.33
1.78	249.72	50.65	515.10	94.17	124.93	23.42
2.37	252.13	49.57	491.31	81.62	125.90	24.40
3.16	248.55	50.57	467.77	68.20	124.93	27.33
4.22	248.54	48.30	442.83	60.31	124.93	25.47
5.62	244.30	49.46	419.96	52.64	125.90	25.38
7.50	244.22	47.93	397.40	49.91	124.93	25.28
10.00	241.57	48.03	378.15	47.76	122.00	27.33
13.34	237.60	46.37	359.03	45.10	122.00	26.35
17.78	236.26	46.38	343.83	45.18	124.93	27.33
23.71	231.88	45.91	328.44	43.13	122.00	23.42
31.62	227.04	43.87	314.87	42.99	124.93	24.40
42.17	222.40	43.31	301.03	41.58	122.00	27.33
56.23	219.16	42.58	288.28	39.99	124.93	25.47
74.99	213.63	42.20	275.75	39.53	125.90	25.38
100.00	206.49	39.91	263.70	37.61	125.90	25.28
133.35	200.51	39.85	251.50	36.39	129.81	24.90
177.83	194.72	38.64	238.11	36.11	128.83	24.72
237.14	187.17	38.25	226.23	35.13	125.90	24.53
316.23	180.78	36.66	214.49	33.97	124.93	24.35
421.70	172.68	35.98	203.75	34.01	125.90	24.17
562.34	166.53	33.45	194.43	31.61	125.90	23.99
749.89	163.46	33.44	187.65	30.53	124.93	23.81
1000.00	161.36	32.44	183.51	30.42	125.90	24.40

Tabla I-2. *Angulo de Fase* (º). Medidas invasivas *No Transmurales* realizadas en animales (cerdos). Valores de los diferentes estados del tejido de miocardio: sano, isquemia aguda y cicatriz.

Frecuencia	Sano		Isquemia Aguda		Cicatriz	
(kHz)	Valor Medio	SD	Valor Medio	SD	Valor Medio	SD
1.00	-1.89	1.67	-8.81	4.44	-2.10	1.70
1.33	-1.89	1.34	-10.11	5.10	-1.90	1.30
1.78	-2.39	1.54	-11.38	5.69	-1.80	1.20
2.37	-2.41	1.31	-12.53	6.05	-1.60	1.50
3.16	-2.86	1.43	-13.37	6.21	-1.30	1.25
4.22	-3.17	1.34	-13.96	6.08	-1.00	1.70
5.62	-3.39	1.35	-14.35	5.74	-0.90	1.50
7.50	-3.80	1.37	-14.45	5.37	-0.80	1.60
10.00	-4.11	1.29	-14.46	4.89	-0.70	1.30
13.34	-4.68	1.28	-14.34	4.35	-0.80	1.30
17.78	-5.15	1.12	-14.15	3.87	-0.70	1.70
23.71	-5.78	1.13	-14.00	3.46	-0.50	1.30
31.62	-6.47	1.01	-13.97	3.13	-0.60	1.20
42.17	-6.88	1.02	-13.92	2.83	-0.70	1.50
56.23	-7.51	0.82	-13.93	2.62	-0.50	1.25
74.99	-8.14	0.87	-14.04	2.39	-0.30	1.70
100.00	-8.80	0.73	-14.17	2.29	-0.50	1.50
133.35	-9.34	1.04	-14.65	2.26	-0.60	1.60
177.83	-9.78	1.01	-14.70	2.05	-0.70	1.50
237.14	-9.97	1.20	-14.49	1.95	-0.90	1.30
316.23	-9.71	1.70	-14.03	1.88	-1.00	1.30
421.70	-9.56	1.94	-13.44	2.01	-1.10	1.42
562.34	-8.46	2.98	-12.46	2.25	-1.00	1.32
749.89	-7.30	3.82	-11.30	2.70	-1.20	1.36
1000.00	-6.63	4.16	-10.72	2.60	-1.20	1.20

Tabla I-3. *Resistividad* (Ω·cm). Medidas invasivas *Transmurales* realizadas en animales (cerdos). Valores de los diferentes estados del tejido de miocardio: sano, isquemia aguda y cicatriz.

Frecuencia	Sano		Isquemia Aguda		Cicatriz	
(kHz)	Valor Medio	SD	Valor Medio	SD	Valor Medio	SD
1.00	278.74	80.54	540.33	260.10	107.11	34.15
1.33	278.46	80.41	534.49	254.11	106.58	33.44
1.78	275.22	79.73	527.45	246.45	107.03	33.75
2.37	275.49	78.36	518.29	237.93	104.86	32.26
3.16	272.60	77.50	506.27	228.60	106.64	33.03
4.22	273.33	76.22	493.05	218.04	106.12	32.61
5.62	268.39	75.87	477.70	206.34	104.48	31.35
7.50	266.86	75.31	460.68	195.28	106.01	32.78
10.00	264.33	74.61	443.31	184.05	104.32	30.98
13.34	260.84	72.21	425.25	172.27	104.14	30.41
17.78	256.20	71.69	406.34	162.12	103.96	30.14
23.71	251.22	68.42	387.62	152.00	101.91	29.25
31.62	248.47	68.49	369.16	142.37	103.33	30.45
42.17	242.19	65.37	350.31	133.96	101.13	28.92
56.23	235.97	64.28	331.62	126.04	100.35	28.75
74.99	228.47	61.71	312.75	118.67	100.03	28.94
100.00	221.55	59.38	293.93	111.83	97.56	26.84
133.35	211.41	56.53	274.84	105.85	97.17	27.75
177.83	202.48	53.69	256.07	99.90	94.86	25.98
237.14	191.60	50.83	237.64	94.60	94.30	26.44
316.23	182.13	48.46	219.92	89.82	92.74	25.78
421.70	170.79	46.09	203.15	85.48	91.59	24.81
562.34	161.10	43.18	187.54	81.67	90.31	24.72
749.89	151.86	41.53	173.65	78.10	89.39	23.80
1000.00	145.93	40.60	161.83	75.02	91.93	27.30

Tabla I-4. *Angulo de Fase* (º). Medidas invasivas *Transmurales* realizadas en animales (cerdos). Valores de los diferentes estados del tejido de miocardio: sano, isquemia aguda y cicatriz.

Frecuencia	Sano		Isquemia Aguda		Cicatriz	
(kHz)	Valor Medio	SD	Valor Medio	SD	Valor Medio	SD
1.00	-2.67	0.77	-3.58	3.28	-5.22	1.03
1.33	-2.51	0.72	-4.46	3.43	-4.02	0.96
1.78	-2.60	0.69	-5.42	3.61	-3.12	0.84
2.37	-2.58	0.71	-6.52	3.71	-2.57	0.76
3.16	-2.76	0.73	-7.73	3.77	-2.16	0.80
4.22	-3.02	0.80	-8.93	3.83	-1.52	1.05
5.62	-3.40	0.64	-10.17	3.74	-1.59	0.95
7.50	-4.04	0.82	-11.35	3.62	-1.64	0.90
10.00	-4.71	0.81	-12.49	3.43	-1.64	1.08
13.34	-5.24	1.04	-13.61	3.19	-1.86	0.97
17.78	-6.13	0.95	-14.72	2.94	-1.93	1.17
23.71	-7.04	1.01	-15.82	2.73	-2.18	1.18
31.62	-8.14	1.03	-16.93	2.65	-2.47	1.13
42.17	-9.15	1.20	-18.07	2.71	-2.67	1.30
56.23	-10.21	1.21	-19.16	2.90	-3.08	1.08
74.99	-11.50	1.25	-20.22	3.17	-3.11	1.44
100.00	-12.46	1.52	-21.23	3.49	-3.22	1.32
133.35	-13.62	1.52	-22.08	3.82	-3.41	1.34
177.83	-14.75	1.71	-22.71	4.04	-3.33	1.70
237.14	-15.44	1.93	-23.07	4.22	-3.32	2.26
316.23	-15.95	2.37	-23.12	4.33	-2.87	3.20
421.70	-16.20	3.29	-22.81	4.36	-2.54	4.61
562.34	-15.94	4.31	-22.08	4.34	-1.53	6.65
749.89	-15.35	5.90	-20.94	4.52	-0.47	9.49
1000.00	-14.10	8.07	-19.28	5.12	1.56	12.73

ANEXO II. PROPIEDADES ELÉCTRICAS PASIVAS

En esta sección se recopilan las propiedades eléctricas de los tejidos utilizados en las simulaciones de los modelos de elementos finitos. Tanto los calculados a partir de las medidas de impedancia especifica transmural para el tejido de miocardio normal isquemia aguda y cicatriz, como el del resto de tejidos empleados en el modelo tomados de la compilación de propiedades dieléctricas de los tejidos de Gabriel and Gabriel 1996.

La Tabla II.1 contiene los valores de conductividad (σ) y permitividad relativa (ε_r) del tejido de miocardio sano, isquemia aguda y cicatriz calculadas a partir de las medidas de la impedancia especifica transmurales, para las 25 frecuencias medidas (1 kHz a 1 MHz).

Los valores de conductividad (σ) (Tabla II.2) y permitividad relativa (ε_r) (Tabla II.3) del tejido muscular, hueso cortical, pulmones en espiración e inspiración y sangre, para las 25 frecuencias medidas (1 kHz a 1 MHz). Obtenidas a partir de la compilación de propiedades dieléctricas de los tejidos de Gabriel and Gabriel et al., 1996.

Tabla II.1. Conductividad (σ, S/m) y permitividad relativa (ε_r) para los diferentes estados del tejido de miocardio (Sano, Isquemia Aguda y Cicatriz)

	Tejidos					
Frecuencia	Sano		Isquemia Aguda		Cicatriz	
(kHz)	σ (S/m)	ε_r	σ (S/m)	ε_r	σ (S/m)	ε_r
1.00	0.388	314927	0.247	157696	1.00	0.000
1.33	0.388	222716	0.248	167734	1.00	0.000
1.78	0.392	174333	0.248	165763	1.00	0.000
2.37	0.391	129706	0.250	161808	1.00	0.000
3.16	0.395	106668	0.254	154526	1.00	0.000
4.22	0.394	86943	0.258	141597	1.00	0.000
5.62	0.400	75575	0.263	128525	1.00	0.000
7.50	0.403	68280	0.270	114131	1.00	0.000
10.00	0.407	60249	0.278	99925	1.00	0.000
13.34	0.412	51167	0.286	86657	1.00	0.000
17.78	0.420	45548	0.298	75128	1.00	0.000
23.71	0.427	40034	0.310	64675	1.00	0.000
31.62	0.433	35234	0.324	55417	1.00	0.000
42.17	0.443	30483	0.340	47734	1.00	0.000
56.23	0.455	26320	0.359	40840	1.00	0.000
74.99	0.470	23012	0.380	34928	1.00	0.000
100.00	0.485	19387	0.405	29862	1.00	0.000
133.35	0.509	16743	0.436	25463	1.00	0.000
177.83	0.530	14164	0.470	21493	1.00	0.000
237.14	0.561	11820	0.511	18019	1.00	0.000
316.23	0.591	9642	0.559	14935	1.00	0.000
421.70	0.630	7872	0.615	12192	1.00	0.000
562.34	0.667	6136	0.679	9756	1.00	0.000
749.89	0.709	4743	0.749	7598	1.00	0.000
1000.00	0.740	3424	0.821	5688	1.00	0.000

Tabla II.2. Conductividad (σ, S/m) para los distintos tejidos empleados en el modelo del tórax

Frecuencia	Músculo	Hueso cortical	Pulmón (espiración)	Pulmón (inspiración)	Sangre
(kHz)	0.321	0.020	0.216	0.080	0.700
1.00	0.325	0.020	0.219	0.081	0.700
1.33	0.328	0.020	0.222	0.083	0.700
1.78	0.331	0.020	0.226	0.085	0.700
2.37	0.333	0.020	0.229	0.086	0.700
3.16	0.336	0.020	0.233	0.088	0.700
4.22	0.337	0.020	0.236	0.090	0.700
5.62	0.339	0.020	0.240	0.092	0.700
7.50	0.341	0.020	0.243	0.093	0.700
10.00	0.342	0.020	0.246	0.095	0.700
13.34	0.344	0.020	0.249	0.096	0.700
17.78	0.346	0.021	0.253	0.098	0.700
23.71	0.348	0.021	0.256	0.100	0.700
31.62	0.350	0.021	0.260	0.102	0.701
42.17	0.353	0.021	0.264	0.103	0.701
56.23	0.357	0.021	0.267	0.105	0.702
74.99	0.362	0.021	0.272	0.107	0.703
100.00	0.369	0.021	0.276	0.110	0.705
133.35	0.379	0.021	0.281	0.112	0.708
177.83	0.393	0.021	0.287	0.114	0.714
237.14	0.410	0.021	0.294	0.117	0.723
316.23	0.432	0.022	0.302	0.121	0.737
421.70	0.456	0.022	0.311	0.125	0.757
562.34	0.480	0.023	0.322	0.130	0.786
749.89	0.503	0.024	0.334	0.136	0.822
1000.00	0.321	0.020	0.216	0.080	0.700

Tabla II.3. Permitividad relativa (ε_r) para los distintos tejidos empleados en el modelo del tórax.

Frecuencia (kHz)	Músculo	Hueso cortical	Pulmón (espiración)	Pulmón (inspiración)	Sangre
1.00	434930	2702	252050	141510	5259
1.33	293270	2263	208130	112770	5258
1.78	197320	1854	167210	88502	5258
2.37	133460	1495	131300	68400	5257
3.16	91455	1195	101360	52228	5256
4.22	63937	956	77418	39577	5255
5.62	45869	770	58829	29901	5253
7.50	33913	628	44683	22614	5251
10.00	25909	522	34044	17174	5248
13.34	20470	442	26083	13126	5244
17.78	16711	382	20128	10111	5239
23.71	14065	337	15662	7857	5232
31.62	12163	303	12297	6163	5222
42.17	10759	277	9745.5	4881	5208
56.23	9688	257	7798.8	3906	5189
74.99	8829	241	6303	3158	5161
100.00	8089	228	5145.3	2581	5120
133.35	7395	217	4241.3	2134	5060
177.83	6684	207	3527.8	1784	4972
237.14	5913	199	2955.9	1509	4843
316.23	5067	190	2487.5	1291	4655
421.70	4174	181	2092.6	1114	4390
562.34	3294	170	1749.2	969	4029
749.89	2498	158	1443.5	844	3569
1000.00	1836	145	1170.5	733	3026

ANEXO III. MÉTODO DE CALIBRACIÓN

En este apartado, se describe el desarrollo del método de calibración para obtener la función de transferencia que caracteriza el sistema de medida. Para ello se ha realizado la caracterización de los electrodos del catéter y del electrodo de referencia mediante circuitos de parámetros eléctricos en PSPICE. Los parámetros se han ajustado para reproducir las medidas experimentales realizadas. También se presenta la caracterización experimental del ruido del sistema.

Método de calibración.

El problema para obtener una calibración de las medidas realizadas se ha planteado de la siguiente forma. Al realizar una medida de impedancia Zx se tiene el esquema mostrado en Figura III-1.

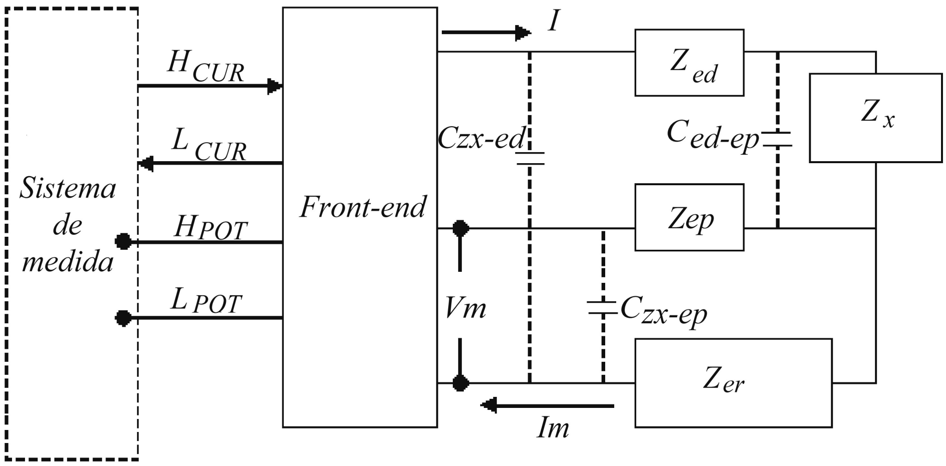

Figura III-1. Esquema de una medida real

Por lo tanto, la impedancia medida por el sistema (Z_{HP}) esta en función de la corriente de retorno al sistema ($L_{CUR} = I_m \cdot H_{I(f)}$) y la tensión medida ($H_{POT} = V_m \cdot H_{V(f)}$):

$$Z_{HP} = \frac{V_m}{I_m} \cdot \frac{H_{v(f)}}{H_{I(f)}}$$

donde la función de transferencia del equipo depende de la función de transferencia de la tensión y la corriente medida:

$$H_{FE(f)} = \frac{H_{v(f)}}{H_{I(f)}}$$

En el caso de considerar que la impedancia de entrada es muy alta e ideal, tenemos que la tensión medida seria directamente proporcional a la impedancia a medir,

$$V_m = I_m Z_x$$

y por lo tanto, la impedancia medida seria proporcional a la impedancia de interés y la función de transferencia del equipo,

$$Z_m = Z_x \cdot H_{FE(f)}$$

Entonces, para conocer la impedancia en cuestión (Z_x) se despejaría de la ecuación anterior

$$Z_x = Z_m \cdot H_{FE(f)}{}^{-1}$$

Pero en el caso de considerar que la impedancia de entrada es muy alta y no es ideal entonces la tensión medida seria,

$$V_m = I_m Z_x \cdot H_{m(f)}$$

donde $H_{m(f)}$ depende de la impedancia de cables, catéter, impedancia de electrodos, etc.

Y la impedancia medida en el sistema HP será

$$Z_{HP} = Z_x \cdot H_{FE(f)} \cdot H_{m(f)}$$

De todo lo anterior tenemos que para conocer la impedancia a medir (Z_x), se debe realizar la caracterización del catéter y del electrodo de referencia utilizado en las medidas así como las capacidades parásitas. De esta forma podremos conocer todas las funciones de transferencia del sistema y encontrar la impedancia de interés.

Caracterización del catéter Blazer II/7Fr/4mm

El catéter presenta las siguientes características a circuito abierto

Circuito Serie: RL donde

$$R_{cat} = 10\,\Omega;\; L_{cat} = 2.8\mu H$$

Circuito Paralelo:

$$C_{cat} = 150\,pF$$

Para conocer las características del electrodo distal (Z_{ed}) y el electrodo proximal (Z_{ep}), se realizan medidas de impedancia a tres hilos, en solución salina, donde la impedancia medida corresponde al terminal de inyección de corriente. Y la medida del electrodo de referencia (Z_{er}) se realiza a dos hilos, entre dos electrodos de referencia de las mismas características. Los resultados medidos en el HP4919A a 10 kHz fueron los siguientes:

$$\begin{aligned} Z_{H_2O} + Z_{ed} &= 29.6\,\Omega \\ Z_{H_2O} + Z_{ep} &= 75.6\,\Omega \\ Z_{H_2O} + 2Z_{er} &= 22.06\,\Omega \\ Z_{H_2O} + Z_{er} &= 13.66\,\Omega \end{aligned}$$

De donde:

$$Z_{er} = 8.4\,\Omega;\; Z_{ed} = 24.3\,\Omega;\; Z_{ep} = 70.34\,\Omega$$

Del espectro de impedancia medida para el electrodo distal y el electrodo proximal, se tiene que la frecuencia de corte es de 3 kHz y 4 kHz respectivamente, por lo tanto, la capacitancia es:

$$C_{ed} = 53\mu F;\; C_{ep} = 39\mu F$$

De esta caracterización se tiene que los electrodos del catéter presentan un comportamiento RC, los valores se detallan en la Tabla III-1.

Tabla III-1. Valores del electrodo distal y proximal.

	Resistencia (Ω)	Capacitancia (μF)
Electrodo Distal	24	53
Electrodo Proximal	70	39

Caracterización de las capacidades de acoplamiento entre la impedancia medida y el catéter

Para obtener las capacidades de acoplamiento entre el cuerpo medido y el catéter, se mide la capacidad del catéter. Para ello, se introduce una longitud aproximada de 60 cm dentro del cilindro con agua en el cual se encuentra el electrodo de referencia. Se realizan distintas medidas variando la longitud del catéter introducido en el cilindro. Los valores medidos a alta frecuencia se detallan en la Tabla III-2.

Tabla III-2. Valores de la capacidad parásita entre los electrodos del catéter y la impedancia a medir. Valores medidos a 1 MHz.

	Capacidad Parásita
Z_x y Electrodo Distal ($C_{zx\text{-}ed}$)	150 pF || 16 MΩ
Z_x y Electrodo Proximal ($C_{zx\text{-}ep}$)	305 pF || 724 Ω
Electrodo Distal y Proximal ($C_{ed\text{-}ep}$)	165 pF || 11 kΩ

También se ha calculado la inductancia mutua entre el cable del electrodo distal y el proximal considerando el retorno a tierra como un plano de masa.

$$\frac{Lm}{l} = \frac{\mu_r \mu_0}{4\pi} \ln\left[1 + \left(\frac{2h}{d}\right)^2\right]$$

y sí $d \to r$ entonces $2h >> d$, considerando un factor de 100, la inductancia mutua es

$$\left.\frac{Lm}{l}\right|_{\frac{2h}{d}=100} = 921 \, {nH}/{m}$$

Si consideramos que la altura es mucho mayor que la distancia entre los cables entonces la inductancia mutua es mayor que 1μH. En el circuito simulado en PSPICE hemos considerado una inductancia de 6 μH.

Por lo tanto el acoplo entre los dos cables provoca una tensión inducida por la interferencia del cable del electrodo distal al cable del electrodo proximal donde se realiza la medida de tensión. La tensión inducida será:

$$va = -Lm\frac{dIs}{dt}$$

Descripción del circuito eléctrico simulado en PSPICE

Una vez que obtuvimos todos los parámetros que intervienen en las medidas experimentales, utilizamos el PSPICE para simular un circuito eléctrico que presentara el mismo comportamiento que las medidas reales en los pacientes y así poder encontrar la función de transferencia del equipo de medida y determinar la impedancia de interés.

El circuito eléctrico se muestra en la Figura III-2 y la nomenclatura utilizada en el circuito se muestra en la Tabla III-3.

Tabla III-3 Nomenclatura del circuito eléctrico simulado en PSPICE.

Símbolo	Descripción
A	Inductancia Mutua
B	Impedancia del cable del electrodo distal
C	Impedancia del electrodo distal
E	Impedancia del electrodo proximal
F	Impedancia del cable del electrodo proximal
G	Impedancia de acoplo entre el electrodo distal y el electrodo proximal
H	Impedancia del cuerpo en interés
I	Impedancia del electrodo de referencia
J	Impedancia de acoplo entre la impedancia a medir y el electrodo proximal en paralelo con la Impedancia de entrada del equipo
K	Impedancia de acoplo entre la impedancia a medir y el electrodo distal

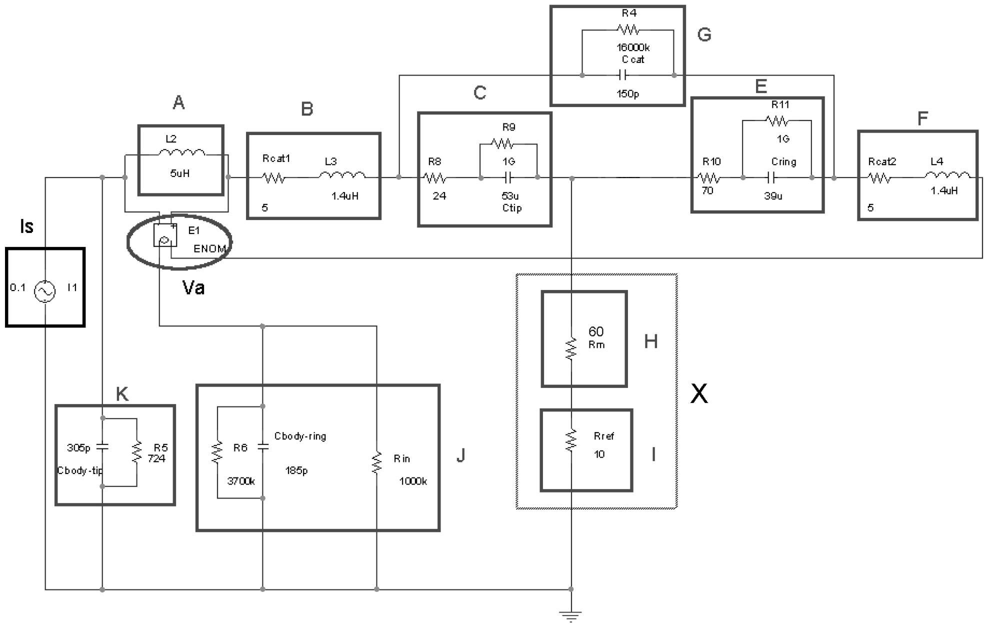

Figura III-2. Caracterización del catéter, modelo eléctrico.

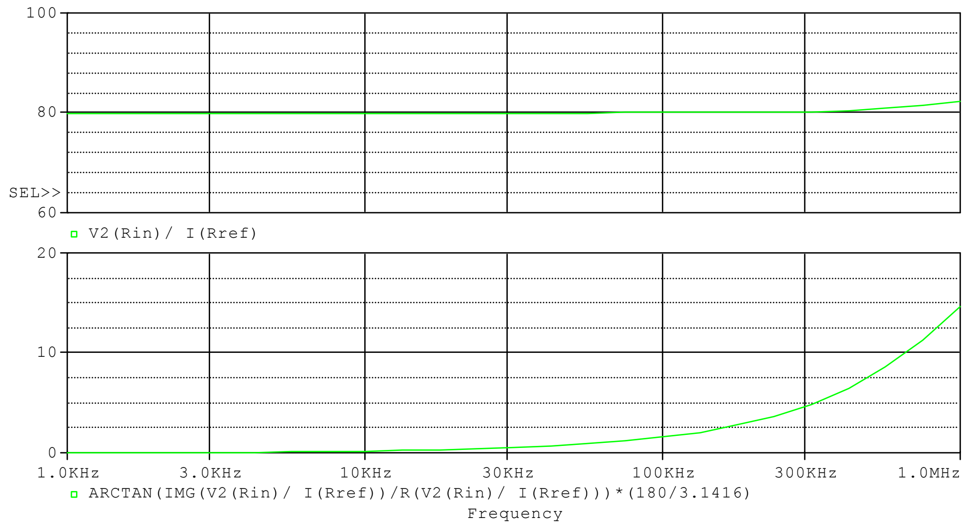

Figura III-3. Respuesta del modelo eléctrico para Zh resistiva

Con este circuito eléctrico y los valores obtenidos de la caracterización del catéter y de las capacitancias parásitas que existían en la medida, obtuvimos una respuesta que representaba las medidas experimentales reales. Empleando una *Zh* y *Zi* puramente resistivas.

Por lo tanto, se realizó el análisis del circuito en función de la impedancia Z_x, la cual equivale a la impedancia a medir más la impedancia del electrodo de referencia

$$Zx = Zh + Zi$$

Tenemos que la impedancia Z_x es

$$Zx = \frac{[Zm(T(f + j) + ge) - a(T(f + g) + e(c + g)) - ejc]}{T(a + j)}$$

donde

$$T = c + e + g$$

Por lo tanto, la impedancia del cuerpo a medir es

$$Zh = Zx - Zi$$

Caracterización del electrodo de referencia empleado en las medidas experimentales en humanos

Al llegar a este punto solo nos falta caracterizar la impedancia del electrodo de referencia utilizado en las medidas (*Zi*). El electrodo de referencia utilizado en las medidas es un electrodo de ablación (3M). La medida de la impedancia del electrodo de ablación (Z_i), se hizo cortando en dos partes iguales un electrodo de ablación ($Z_{1,2}$). Se colocaron en el brazo derecho de un voluntario en la parte interna y externa del brazo. Se realizo una medida a dos electrodos con el analizador de impedancias (HP4192A), considerando que la impedancia del electrodo de ablación es mayor que la impedancia del brazo (Z_b) por lo tanto se desprecia.

$$Z_m = 2Z_{1,2} + Z_b$$

La impedancia total del electrodo de ablación es $Z_i = \frac{1}{2} Z_{1,2}$

Calculando la impedancia del *Zi* obtenemos el espectro de impedancia de este electrodo Figura III-4. Para encontrar *Zh* se resta el valor de *Zi* a cada una de las frecuencias de interés como un valor fijo ya que no tenemos esta medida en cada uno de los pacientes.

$$Zh_{f_i} = Zx_{f_i} - Zi_{f_i}$$

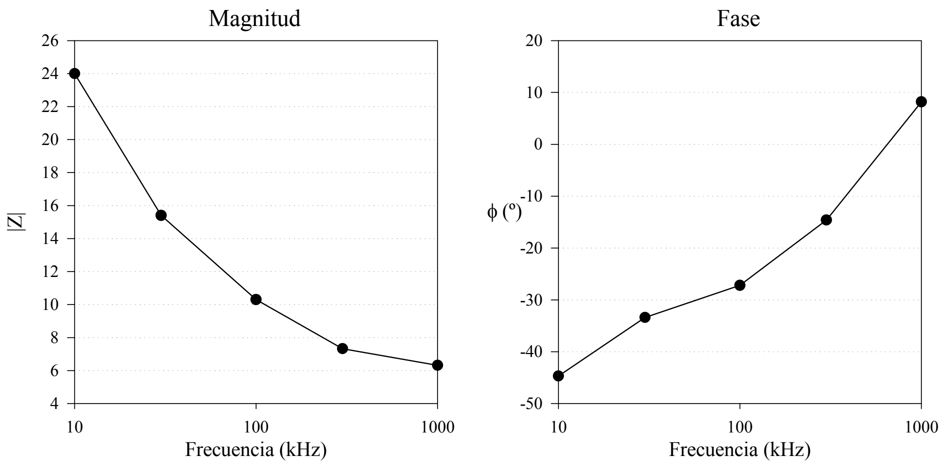

Figura III-4. Espectro de la impedancia del electrodo de referencia utilizado en las medidas en humanos.

De esta forma una calibración que nos permite corregir los artefactos de alta frecuencia (calculando *Zx*) y reducir el la impedancia del electrodo de referencia (calculando *Zh*) que tenia una influencia a baja frecuencia (10 kHz).

ANEXO IV. INCREMENTO DE IMPEDANCIA DEBIDO A LA RESPIRACIÓN

En este anexo, se muestran los resultados de las simulaciones del modelo de elementos finitos del tórax debido al cambio de respiración, posición del electrodo de referencia y posición del catéter. Se han dividido en tres tablas correspondientes a las tres distintas posiciones del electrodo de referencia ERA (Tabla IV-1), ERP (Tabla IV-2) y ERL (Tabla IV-3). En cada una de las tablas se muestran el incremento de magnitud ($\Delta|Z|$) entre espiración e inspiración, los incrementos relativos ($\Delta|Z|/|Z|$ (%)) con respecto a espiración y las diferencias de fase ($\Delta\phi = \phi$ inspiración – ϕ espiración), para el tejido sano, la isquemia aguda y la cicatriz para los dos métodos de medida, 3EM y 2EM.

Tabla IV-3.Variaciones de la respiración. Electrodo de Referencia Anterior (ERA).

ERA						
sano			**3EM**			
	posición del cateter		*0*	*1*	*2*	*3*
	1 kHz	Δ|Z|	5.4	5.4	2.8	4.3
		Δ|Z|/|Z| (%)	10.6	10.5	5.7	9.1
	1 MHz	Δϕ	-0.6	-0.6	-0.3	-0.5
			2EM			
	posición del cateter		*0*	*1*	*2*	*3*
	1 kHz	Δ|Z|	5.9	6.3	2.7	4.6
		Δ|Z|/|Z| (%)	5.5	5.6	2.5	4.4
	1 MHz	Δϕ	-0.3	-0.3	-0.1	-0.2
isquemia			**3EM**			
	posición del cateter		*0*	*1*	*2*	*3*
	1 kHz	Δ|Z|	5.4	5.4	2.8	4.3
		Δ|Z|/|Z| (%)	10.2	10.0	5.5	8.8
	1 MHz	Δϕ	-0.6	-1	-0.3	-0.5
			2EM			
	posición del cateter		*0*	*1*	*2*	*3*
	1 kHz	Δ|Z|	5.9	6.2	2.7	4.6
		Δ|Z|/|Z| (%)	5.3	5.3	2.4	4.4
	1 MHz	Δϕ	-0.6	-0.3	-0.1	-0.2
cicatriz			**3EM**			
	posición del cateter		*0*	*1*	*2*	*3*
	1 kHz	Δ|Z|	5.3	5.2	2.9	4.2
		Δ|Z|/|Z| (%)	11.1	11.2	5.8	9.0
	1 MHz	Δϕ	-0.6	-0.6	-0.3	-0.5
			2EM			
	posición del cateter		*0*	*1*	*2*	*3*
	1 kHz	Δ|Z|	5.8	5.9	2.7	4.4
		Δ|Z|/|Z| (%)	5.7	6.0	2.5	4.4
	1 MHz	Δϕ	-0.3	-0.3	-0.1	-0.2

Tabla IV-2. Electrodo de Referencia Posterior.

ERP						
sano			**3EM**			
	posición del cateter		*0*	*1*	*2*	*3*
	1 kHz	Δ|Z|	11	12	9	10
		Δ|Z|/|Z| (%)	15	14	11	13
	1 MHz	Δϕ	-0.7	-0.7	-0.5	-0.6
			2EM			
	posición del cateter		*0*	*1*	*2*	*3*
	1 kHz	Δ|Z|	12	13	9	11
		Δ|Z|/|Z| (%)	8	8	6	7
	1 MHz	Δϕ	-0.4	-0.4	-0.3	-0.3
isquemia			**3EM**			
	posición del cateter		*0*	*1*	*2*	*3*
	1 kHz	Δ|Z|	11	12	9	10
		Δ|Z|/|Z| (%)	14	**14**	11	13
	1 MHz	Δϕ	-0.7	**-0.7**	-0.5	-0.6
			2EM			
	posición del cateter		*0*	*1*	*2*	*3*
	1 kHz	Δ|Z|	12	13	9	11
		Δ|Z|/|Z| (%)	8	8	6	7
	1 MHz	Δϕ	-0.4	-0.4	-0.3	-0.4
cicatriz			**3EM**			
	posición del cateter		*0*	*1*	*2*	*3*
	1 kHz	Δ|Z|	11	11	9	10
		Δ|Z|/|Z| (%)	16	15	11	14
	1 MHz	Δϕ	-0.8	-0.8	-0.5	-0.6
			2EM			
	posición del cateter		*0*	*1*	*2*	*3*
	1 kHz	Δ|Z|	12	13	9	11
		Δ|Z|/|Z| (%)	9	9	6	7
	1 MHz	Δϕ	-0.4	-0.5	-0.3	-0.3

Tabla IV-3. Electrodo de Referencia Lateral

ERL						
sano			**3EM**			
	posición del cateter		*0*	*1*	*2*	*3*
	1 kHz	Δ|Z|	14	13	10	12
		Δ|Z|/|Z| (%)	19	17	14	17
	1 MHz	Δϕ	-0.9	-0.8	-0.6	-0.8
			2EM			
	posición del cateter		*0*	*1*	*2*	*3*
	1 kHz	Δ|Z|	15	15	10	13
		Δ|Z|/|Z| (%)	10	9	7	9
	1 MHz	Δϕ	-0.5	-0.5	-0.3	-0.4
isquemia			**3EM**			
	posición del cateter		*0*	*1*	*2*	*3*
	1 kHz	Δ|Z|	13	13	10	12
		Δ|Z|/|Z| (%)	18	16	13	16
	1 MHz	Δϕ	-0.9	-0.8	-0.6	-0.8
			2EM			
	posición del cateter		*0*	*1*	*2*	*3*
	1 kHz	Δ|Z|	14	15	10	13
		Δ|Z|/|Z| (%)	10	9	7	9
	1 MHz	Δϕ	-0.5	-0.4	-0.3	-0.4

Con los datos obtenidos de las simulaciones de tejido sano e isquemia aguda podíamos anticipar que los cambios serian de la misma magnitud para esta posición del electrodo de referencia. Por lo tanto, para cicatriz solamente se simuló la posición 0, los resultados obtenidos son:

Cicatriz	Posición del cateter		**0**	
	método		*3EM*	2EM
	1 kHz	Δ|Z|	14	15
		Δ|Z|/|Z| (%)	20	11
	1 MHz	Δϕ	-1.1	-0.5

(1994) Diagnosing and managing unstable angina. Agency for Health Care Policy and Research. *Clin Pract Guidel Quick Ref Guide Clin*, **10**, 1-25.

Alpert, J.S., Antman, E., Apple, F., Armstrong, P.W., Bassand, J.P., de Luna, A.B., Beller, G., Breithardt, G., et al., (2000) Myocardial infarction redefined - A consensus document of the Joint European Society of Cardiology/American College of Cardiology Committee for the Redefinition of Myocardial Infarction. *European Heart Journal*, **21**, 1502-1513.

Avitall, B., Mughal, K., Hare, J., Helms, R. and Krum, D. (1997) The effects of electrode-tissue contact on radiofrequency lesion generation. *Pace-Pacing and Clinical Electrophysiology*, **20**, 2899-2910.

Baarends, E.M., Lichtenbelt, W.D.V., Wouters, E.F.M. and Schols, A. (1998) Body-water compartments measured by bio-electrical impedance spectroscopy in patients with chronic obstructive pulmonary disease. *Clinical Nutrition*, **17**, 15-22.

Bao, J.Z., Davis, C.C. and Schmukler, R.E. (1993) Impedance Spectroscopy of Human Erythrocytes - System Calibration and Nonlinear Modeling. *IEEE Transactions on Biomedical Engineering*, **40**, 364-378.

Bocchi, E.A., Mocelin, A.O., deMoraes, A.V., Menegheti, C., Higuchi, M.D., Bacal, F., Stolf, N., Bellotti, G. and Pileggi, F. (1997) Comparison between two strategies for rejection detection after heart transplantation: Routine endomyocardial biopsy versus gallium-67 cardiac imaging. *Transplantation Proceedings*, **29**, 586-588.

Bolton, M.P., Ward, L.C., Khan, A., Campbell, I., Nightingale, P., Dewit, O. and Elia, M. (1998) Sources of error in bioimpedance spectroscopy. *Physiological Measurement*, **19**, 235-245.

Borsic, A., McLeod, C., Lionheart, W. and Kerrouche, N. (2001) Realistic 2D human thorax modelling for EIT. *Physiological Measurement*, **22**, 77-83.

Bragos, R. (1997) Contribuciò a la caracterització de teixits i sistemes biològics mitjançant tècniques d'espectrocòpia d'impedància elèctrica. *Departament d'enginyeria electrònica*. Universitat Politècnica de Catalunya, Barcelona, España.

Bragos, R., A. Yañez, P.J. Riu, M. Warren, A. Carreño and J. Cinca. Espectro de la impedancia del miocardioi porcino in situ durante la isquemia Parte I: sistema de medida. *XIV Congreso Anual de la Sociedad Española de Ingeniera Biomédica*, pp. 97-99.

Bragos, R., Blanco-Enrich, R., Casas, O. and Rosell, J. (2001a) Characterisation of dynamic biologic systems using multisine based impedance spectroscopy. *Instrumentation and Measurement Technology Conference, 2001. IMTC 2001. Proceedings of the 18th IEEE*, Vol. 1, pp. 44-47.

Bragos, R., Casas, O., Rosell, J., Riu, P.J., Rodriguez-Sinovas, A. and Cinca, J. (2001b) Detection of Healed Myocardium Scar In Pigs Measuring The Electrical Impedance Spectrum With A Percutaneous Catheter. *XI ICEBI, International Conference on Electrical Bio-Impedance*, Oslo, Norway, pp. 63-66.

Bragos, R., Casas, O., Rosell, J., Warren, M., Tresanchez, M., Carreño, A., Rodriguez-Sinovas, A. and Cinca, J. (1999) In vivo detection of healed myocardium scar in pigs measuring the electrical impedance spectrum with an intracavitary catheter. *5th Conference of the European Society for Engineering and Medicine*, Barcelona, Spain, pp. 487-488.

Bragos, R., Povill, R. and Riu, P. (1994) Applicability of the three coefficiente calibration technique in EIT. *6th European Community Workshop on Electrical Empedance Tomography*, Ankara, Turkey, pp. 49-50.

Bragos, R., Riu, P., Cairo, J., Montesinos, J.L. and Tinto, A. (1995) On-line estimation of biomass in free and immobilized cell cultures using two-frequency measurements. *IX International Conference on Electrical Bio-Impedance*, Heidelberg, Germany, pp. 59-62.

Bragos, R., Riu, P.J., Warren, M., Tresanchez, M., Carreno, A. and Cinca, J. (1996) Changes in myocardial impedance spectrum during acute ischemia in the in-situ pig heart. *Engineering in Medicine and Biology Society, 1996. Bridging Disciplines for Biomedicine. Proceedings of the 18th Annual International Conference of the IEEE*, Vol. 5, pp. 1953-1954.

Bragos, R., Rosell, J., Casas, O., Riu, P. and Cinca, J. (2002) Transcatheter detection of healed myocardial infarction in pigs using electrical impedance and motion induced changes. *EMBEC'02*, Vienna.

Brown, B.H., Barber, D.C., Morice, A.H. and Leathard, A.D. (1994) Cardiac and respiratory related electrical impedance changes in the human thorax. *Biomedical Engineering, IEEE Transactions on*, **41**, 729-734.

Cao, H., Speidel, M.A., Tsai, J.Z., Van Lysel, M.S., Vorperian, V.R. and Webster, J.G. (2002a) FEM analysis of predicting electrode-myocardium contact from RF cardiac catheter ablation system impedance. *IEEE Transactions on Biomedical Engineering*, **49**, 520-526.

Cao, H., Tungjitkusolmun, S., Choy, Y.B., Tsai, J.Z., Vorperian, V.R. and Webster, J.G. (2002b) Using electrical impedance to predict catheter-endocardial contact during RF cardiac ablation. *IEEE Transactions on Biomedical Engineering*, **49**, 247-253.

Cao, H., Vorperian, V.R., Tsai, J.Z., Tungjitkusolmun, S., Woo, E.J. and Webster, J.G. (2000) Temperature measurement within myocardium during in vitro RF catheter ablation. *IEEE Transactions on Biomedical Engineering*, **47**, 1518-1524.

Casas, O. (1998) Contribución a la obtención de imágenes paramétricas en tomografía de impedancia eléctrica para la caracterización de tejidos biológicos. *Engenieria Electrónica*. Universidad Politécnica de Cataluña, Barcelona.

Casas, O., Bragos, R., Riu, P.J., Rosell, J., Tresanchez, M., Warren, M., Rodriguez-Sinovas, A., Carreno, A. and Cinca, J. (1999) In vivo and in situ ischemic tissue characterization using electrical impedance spectroscopy. In *Electrical Bioimpedance Methods: Applications to Medicine and Biotechnology*, Vol. 873, pp. 51-58.

Casas, O., Bragos, R., Riu, P.J., Rosell, J., Tresanchez, M., Warren, M., Rodriguez-Sinovas, A., Carreño, A. and Cinca, J. (1998) In-Vivo and in-situ ischemic tissue characterisation using electrical impedance spectroscopy. *X International Conference on Electrical Bio-Impedance*, Barcelona, Spain, pp. 69-72.

Chu, E., Fitzpatrick, A., Chin, M., Sudhir, K., Yock, P. and Lesh, M. (1994) Radiofrequency catheter ablation guided by intracardiac echocardiography. *Circulation*, **89**, 1301-1305.

Cinca, J., Warren, M., Carreno, A., Tresanchez, M., Armadans, L., Gomez, P. and SolerSoler, J. (1997) Changes in myocardial electrical impedance induced by coronary artery occlusion in pigs with and without preconditioning - Correlation with local ST-segment potential and ventricular arrhythmias. *Circulation*, **96**, 3079-3086.

Cinca, J., Warren, M., Rodriguez-Sinovas, A., Tresanchez, M., Carreno, A., Bragos, R., Casas, O., Domingo, A. and Soler-Soler, J. (1998) Passive transmission of ischemic ST segment changes in low electrical resistance myocardial infarct scar in the pig. *Cardiovascular Research*, **40**, 103-112.

Cohen, K.P., Ladd, W.M., Beams, D.M., Sheers, W.S., Radwin, R.G., Tompkins, W.J. and Webster, J.G. (1997) Comparison of impedance and inductance ventilation sensors on adults during breathing, motion, and simulated airway obstruction. *Ieee Transactions on Biomedical Engineering*, **44**, 555-566.

Cornish, B.H., Jacobs, A., Thomas, B.J. and Ward, L.C. (1999) Optimizing electrode sites for segmental bioimpedance measurements. *Physiological Measurement*, **20**, 241-250.

Critchley, L.A.H., Calcroft, R.M., Tan, P.Y.H., Kew, J. and Critchley, J. (2000) The effect of lung injury and excessive lung fluid, on impedance cardiac output measurements, in the critically ill. *Intensive Care Medicine*, **26**, 679-685.

Ellenby, M.I., Small, K.W., Wells, R.M., Hoyt, D.J. and Lowe, J.E. (1987) Online Detection of Reversible Myocardial Ischemic-Injury by Measurement of Myocardial Electrical-Impedance. *Annals of Thoracic Surgery*, **44**, 587-597.

Ellman, P., Ronson, R. and Kron, I. (2003) Modern concepts in heart transplantation. *Journal of long-term effects of medical implants*, **13**, 465-483.

Endt, P., Montonen, J., Makijarvi, M., Nenonen, J., Steinhoff, U., Trahms, L. and Katila, T. (2000) Identification of post-myocardial infarction patients with ventricular tachycardia by time-domain intra-QRS analysis of signal-averaged electrocardiogram and magnetocardiogram. *Medical & Biological Engineering & Computing*, **38**, 659-665.

Esberg, D. and Greenspon, A.J. (2001) Avoiding complications of catheter ablation: a review of the current state of the art. *J Invasive Cardiol*, **13**, 323-327.

Everett, J.E., Palmer, M.N., Jessurun, J. and Shumway, S.J. (1996) Noninvasive diagnosis of cardiac allograft rejection in an orthotopic canine model. *Annals of Thoracic Surgery*, **62**, 1337-1340.

Eyuboglu, B.M., Brown, B.H. and Barber, D.C. (1989) In vivo imaging of cardiac related impedance changes. *Engineering in Medicine and Biology Magazine, IEEE*, **8**, 39-45.

Faes, T.J.C., van der Meij, H.A., de Munck, J.C. and Heethaar, R.M. (1999) The electric resistivity of human tissues (100 Hz-10 MHz): a meta-analysis of review studies. *Physiological Measurement*, **20**, R1-R10.

Fallert, M.A., Mirotznik, M.S., Downing, S.W., Savage, E.B., Foster, K.R., Josephson, M.E. and Bogen, D.K. (1993) Myocardial Electrical-Impedance Mapping of Ischemic Sheep Hearts and Healing Aneurysms. *Circulation*, **87**, 199-207.

Foster, K. and Schwan, H.P. (1996) Dielectric properties of tissues. In Polk, C.a.P., E. (ed.), *Handbook of Biological Effects of electromagnetic Fields*. Boca Raton: CRC Press, pp. 25-102.

Frerichs, I. (2000) Electrical impedance tomography (EIT) in applications related to lung and ventilation: a review of experimental and clinical activities. *Physiological Measurement*, **21**, R1-R21.

Gabriel, C. and Gabriel, S. (1996) Compilation of the Dielectric Properties of Body Tissues at RF and Microwave Frecuencies. Armstrong Laboratory (AFMC); Occupational and Environmental Health Directorate Radiofrequency Radiation Division, Texas, USA.

Gabriel, C., Gabriel, S. and Corthout, E. (1996a) The dielectric properties of biological tissues .1. Literature survey. *Physics in Medicine and Biology*, **41**, 2231-2249.

Gabriel, S., Lau, R.W. and Gabriel, C. (1996b) The dielectric properties of biological tissues .2. Measurements in the frequency range 10 Hz to 20 GHz. *Physics in Medicine and Biology*, **41**, 2251-2269.

Gabriel, S., Lau, R.W. and Gabriel, C. (1996c) The dielectric properties of biological tissues .3. Parametric models for the dielectric spectrum of tissues. *Physics in Medicine and Biology*, **41**, 2271-2293.

García-González, M.A., Ramos-Castro, J., Salazar, Y., Bragos, R., Bayés-Genis, A., Rosell, J. and Cinca, J. (2003) Obtención del perfil de temperatura intracardiaco y su variación con la respiración en modelos porcinos anestesiados. *Congreso Anual de la Sociedad Española de Ingeniería Biomédica*, Mérida, España., pp. 187-190.

Geddes, L.A. (1989) Detection of physiological events by impedance. In *Principles of Applied Biomedical Instrumentation*. Wiley Interscience, New York, Vol. 1, pp. 276-410.

Geddes, L.A. and Baker, L.E. (1967) Specific Resistance of Biological Material-a Compendum of Data for Biomedical Engineer and Physiologist. *Medical & Biological Engineering*, **5**, 271-&.

Gersing, E. (1998) Impedance spectroscopy on living tissue for determination of the state of organs. *Bioelectrochemistry and Bioenergetics*, **45**, 145-149.

Gersing, E., Bach, F., Gapikowski, H., Meissner, A., Schmidt, G. and Bretschneider, H.J. (1989) Electric impedance spectroscopy in organ conservation research. In Nikiforidis, G., Pallikarakis, N. and Proimos, B. (eds.), *V Mediterranean Conference on Medical and Biological Engineering*, Patras, Greece, pp. 164-165.

Gheorghiu, M., Gersing, E. and Gheorghiu, E. (1999) Quantitative analysis of impedance spectra of organs during ischemia. In *Electrical Bioimpedance Methods: Applications to Medicine and Biotechnology*, Vol. 873, pp. 65-71.

Gill, J.B., Cairns, J.A., Roberts, R.S., Costantini, L., Sealey, B.J., Fallen, E.F., Tomlinson, C.W. and Gent, M. (1996) Prognostic importance of myocardial ischemia detected by ambulatory monitoring early after acute myocardial infarction. *New England Journal of Medicine*, **334**, 65-70.

Gradek, W.Q., D'Amico, C., Smith, A.L., Vega, D. and Book, W.M. (2001) Routine surveillance endomyocardial biopsy continues to detect significant rejection late after heart transplantation. *Journal of Heart and Lung Transplantation*, **20**, 497-502.

Grauhan, O., Muller, J., Knosalla, C., Cohnert, T., Siniawski, H., Volk, H.D., Fietze, E., Kupetz, W. and Hetzer, R. (1996) Electric myocardial impedance registration in humoral rejection after heart transplantation. *Journal of Heart and Lung Transplantation*, **15**, 136-143.

Greenspon, A.J. (2000) Advances in catheter ablation for the treatment of cardiac arrhythmias. *IEEE Transactions on Microwave Theory and Techniques*, **48**, 2670-2675.

Grimnes, S. and Martinsen, O.G. (2000) *Bioimpedance and Bioelectricity Basics.* Academic Pres.

Hahn, G., Sipinkova, I., Baisch, F. and Hellige, G. (1995) Changes in the Thoracic Impedance Distribution under Different Ventilatory Conditions. *Physiological Measurement*, **16**, A161-A173.

Haines, D.E. and Verow, A.F. (1990) Observations on Electrode-Tissue Interface Temperature and Effect on Electrical-Impedance During Radiofrequency Ablation of Ventricular Myocardium. *Circulation*, **82**, 1034-1038.

Helguera, M., Pinski, S., Elizalde, G., Corrado, G., Schargrodsky, H. and Bazzino, O. (1998) Ablación por radiofrecuencia de arritmias cardiacas. *Nexo*, **18**.

Herlitz, J., Karlson, B.W., Lindqvist, J. and Sjolin, M. (2002) Characteristics and long-term outcome of patients with acute chest pain or other symptoms raising suspicion of acute myocardial infarction in relation to whether they were hospitalized or directly discharged from the emergency department. *Coronary Artery Disease*, **13**, 37-43.

Howie, M.B., Dzwonczyk, R. and McSweeney, T.D. (2001) An evaluation of a new two-electrode myocardial electrical impedance monitor for detecting myocardial ischemia. *Anesthesia and Analgesia*, **92**, 12-18.

Hoyt, R.H., Cohen, M.L. and Saffitz, J.E. (1989) Distribution and 3-Dimensional Structure of Intercellular-Junctions in Canine Myocardium. *Circulation Research*, **64**, 563-574.

Hyttinen, J., Kauppinen, P., Koobi, T. and Malmivuo, J. (1997) Importance of the tissue conductivity values in modelling the thorax as a volume conductor. In *Proceedings of the 19th Annual International Conference of the Ieee Engineering in Medicine and Biology Society, Vol 19, Pts 1-6 - Magnificent Milestones and Emerging Opportunities in Medical Engineering.* I E E E, New York, Vol. 19, pp. 2082-2085.

Ishikawa, M., Hirose, H., Sasaki, E., Bando, M., Mori, Y. and Murakawa, S. (1996) Evaluation of myocardial viability during simple cold storage with the use of electrical properties in broad frequencies. *The Journal of heart and lung transplantation*, **15**, 1005-1011.

Jain, M.K., Tomassoni, G., Riley, R.E. and Wolf, P.D. (1998) Effect of skin electrode location on radiofrequency ablation lesions: An in vivo and a three-dimensional finite element study. *Journal of Cardiovascular Electrophysiology*, **9**, 1325-1335.

Jain, M.K. and Wolf, P.D. (2000) A three-dimensional finite element model of radiofrequency ablation with blood flow and its experimental validation. *Annals of Biomedical Engineering*, **28**, 1075-1084.

Jarverud, K., Ollmar, S. and Brodin, L.A. (2002) Analysis of the O-wave in acute right ventricular apex impedance measurements with a standard pacing lead in animals. *Medical & Biological Engineering & Computing*, **40**, 512-519.

Jereczek, M., Andresen, D., Schroder, J., Voller, H., Bruggemann, T., Deutschmann, C. and Schroder, R. (1993) Prognostic Value of Ischemia During Holter Monitoring and Exercise Testing after Acute Myocardial-Infarction. *American Journal of Cardiology*, **72**, 8-13.

Jesse, R.L. and Kontos, M.C. (1997) Evaluation of Chest Pain in the Emergency Department. *Current Problems in Cardiology*, **22**, 154-236.

Jorgenson, D.B., Haynor, D.R., Bardy, G.H. and Kim, Y.M. (1995) Computational Studies of Transthoracic and Transvenous Defibrillation in a Detailed 3-D Human Thorax Model. *Ieee Transactions on Biomedical Engineering*, **42**, 172-184.

Jossinet, J. (1988) A hardware design for imaging the electrical impedance of the breast. *Clinical physics and physiological measurement*, **9**, 25-28.

Karlon, W.J., Lehr, J.L. and Eisenberg, S.R. (1994) Finite-Element Models of Thoracic Conductive Anatomy - Sensitivity to Changes in Inhomogeneity and Anisotropy. *Ieee Transactions on Biomedical Engineering*, **41**, 1010-1017.

Kerner, T.E., Paulsen, K.D., Hartov, A., Soho, S.K. and Poplack, S.P. (2002) Electrical impedance spectroscopy of the breast: clinical imaging results in 26 subjects. *Medical Imaging, IEEE Transactions on*, **21**, 638-645.

Khambete, N.D., Brown, B.H. and Smallwood, R.H. (2000) Movement artefact rejection in impedance pneumography using six strategically placed electrodes. *Physiological Measurement*, **21**, 79-88.

Kim, D.W., Kim, N.H., Kim, W.K. and Park, S.H. (1989) Current Distribution in a 3-D Thorax Model for Impedance Cardiography. In *Images of the Twenty-First Century, Pts 1-6*. I E E E, New York, Vol. 11, pp. 1235-1236.

Kleber, A.G., Riegger, C.B. and Janse, M.J. (1987) Electrical Uncoupling and Increase of Extracellular Resistance after Induction of Ischemia in Isolated, Arterially Perfused Rabbit Papillary-Muscle. *Circulation Research*, **61**, 271-279.

Ko, W.C., Huang, S.K.S., Lin, J.L., Shau, W.Y., Lai, L.P. and Chen, P.H. (2001) New method for predicting efficiency of heating by measuring bioimpedance during radiofrequency catheter ablation in humans. *Journal of Cardiovascular Electrophysiology*, **12**, 819-823.

Kontos, M.C., Anderson, F.P., Schmidt, K.A., Ornato, J.P., Tatum, J.L. and Jesse, R.L. (1999) Early diagnosis of acute myocardial infarction in patients without ST-segment elevation. *The American Journal of Cardiology*, **83**, 155-158.

Kornowski, R., Hong, M.K., Gepstein, L., Goldstein, S., Ellahham, S., Ben-Haim, S.A. and Leon, M.B. (1998) Preliminary animal and clinical experiences using an electromechanical endocardial mapping procedure to distinguish infarcted from healthy myocardium. *Circulation*, **98**, 1116-1124.

Kunst, P.W.A., Noordegraaf, A.V., Raaijmakers, E., Bakker, J., Groeneveld, A.B.J., Postmus, P.E. and de Vries, P. (1999) Electrical impedance tomography in the assessment of extravascular lung water in noncardiogenic acute respiratory failure. *Chest*, **116**, 1695-1702.

Lafer, G., Tilg, B., Wach, P. and Rucker, W. (1997) Simulation of the body surface potential map using a realistic heart and thorax model. In *Proceedings of the 18th Annual International Conference of the Ieee Engineering in Medicine and Biology Society, Vol 18, Pts 1-5*. I E E E, New York, Vol. 18, pp. 1417-1418.

Levi, D.S., DeConde, A.S., Fishbein, M.C., Burch, C., Alejos, J.C. and Wetzel, G.T. (2004) The yield of surveillance endomyocardial biopsies as a screen for cellular rejection in pediatric heart transplant patients. *Pediatric Transplantation*, **8**, 22-28.

Lingwood, B.E., Coghlan, J.P., Ward, L.C., Charles, B.G. and Colditz, P.B. (2000) Measurement of extracellular fluid volume in the neonate using multiple frequency bio-impedance analysis. *Physiological Measurement*, **21**, 251-262.

Littwitz, C., Ragheb, T. and Geddes, L.A. (1990) Cell Constant of the Tetrapolar Conductivity Cell. *Medical & Biological Engineering & Computing*, **28**, 587-590.

Lundmark, E.V., Oldenburg, J.T. and Sharma, A.D. (1997) New method for assessing tissue contact before and during radiofrequency catheter ablation. *Circulation*, **96**, 794-794.

Luo, S., Afonso, V.X., Webster, J.G. and Tompkins, W.J. (1992) The Electrode System in Impedance-Based Ventilation Measurement. *Ieee Transactions on Biomedical Engineering*, **39**, 1130-1141.

Luo, S., Tompkins, W.J. and Webster, J.G. (1994) Cardiogenic Artifact Cancellation in Apnea Monitoring. In *Proceedings of the 16th Annual International Conference of the Ieee Engineering in Medicine and Biology Society - Engineering Advances: New Opportunities for Biomedical Engineers, Pts 1&2*. I E E E, New York, pp. 968-969.

Mahrholdt, H., Wagner, A., Judd, R.M. and Sechtem, U. (2002) Assessment of myocardial viability by cardiovascular magnetic resonance imaging. *European Heart Journal*, **23**, 602-619.

Martínez-Sánchez, C., Chuquiure-Valenzuela, E., López-Rodríguez, M.C. and Juárez-Herrera, U. (2000) Urgencias Cardiológicas II. In Intersistemas, S.A.d.C.V. (ed.), *PAC Cardio-2 Programa de Actualización continua para el cardiólogo*, México, Vol. 10.

Martinsen, O.G., Grimnes, S. and Karlsen, J. (1995) Electrical Methods for Skin Moisture Assessment. *Skin Pharmacology*, **8**, 237-245.

Mayotte, M.J., Webster, J.G. and Tompkins, W.J. (1994) A Comparison of Electrodes for Potential Use in Pediatric Infant Apnea Monitoring. *Physiological Measurement*, **15**, 459-467.

Mayotte, M.J., Webster, J.G. and Tompkins, W.J. (1996) Reduction of motion artefacts during paediatric/infant apnoea monitoring. *Medical & Biological Engineering & Computing*, **34**, 93-96.

Mehra, M.R., Uber, P.A., Potluri, S., Ventura, H., Scott, R.L. and Park, M.H. (2003) Elevated B-type natriuretic peptide predicts allograft failure and mortality after heart transplantation. *Circulation*, **108**, 388-388.

Menown, I.B., Allen, J., Anderson, J.M. and Adgey, A.A. (2000) Early diagnosis of right ventricular or posterior infarction associated with inferior wall left ventricular acute myocardial infarction. *American Heart Journal*, **85**, 934-938.

Merck, M. (2001) 198/ Procedimientos de diagnóstico cardiovascular. In Merck Sharp & Dohme de España, S.A. (ed.), *Manual Merck de información medica para el hogar*. Grupo MSD, Madrid, España.

Miller, J.M. (2002) Catheter ablation of arrhythmias. *Circulation*, **106**, E203-E205.

Morady, F. (1999) Drug therapy - Radio-frequency ablation as treatment for cardiac arrhythmias. *New England Journal of Medicine*, **340**, 534-544.

Morillas, P.J., Cabades, A., Bertomeu, V., Echanove, I., Colomina, F., Cebrian, J., Perez, G., Mota, A., Sanchez, F.J. and Sanz, J.C. (2002) Acute myocardial infarction in patients under 45 years. *Revista Espanola De Cardiologia*, **55**, 1124-1131.

Morucci, J.P. and Rigaud, B. (1996) Bioelectrical impedance techniques in medicine .3. Impedance imaging - Third section: Medical applications. *Critical Reviews in Biomedical Engineering*, **24**, 655-677.

Nakagawa, H., Wittkampf, F.H.M., Yamanashi, W.S., Pitha, J.V., Imai, S., Campbell, B., Arruda, M., Lazzara, R. and Jackman, W.M. (1998) Inverse Relationship Between Electrode Size and Lesion Size During

Radiofrequency Ablation With Active Electrode Cooling. *Circulation*, **98**, 458-465.

Nath, S., DiMarco, J.P., Gallop, R.G., McRury, I.D. and Haines, D.E. (1996) Effects of dispersive electrode position and surface area on electrical parameters and temperature during radiofrequency catheter ablation. *American Journal of Cardiology*, **77**, 765-&.

Nierman, D.M., Eisen, D.I., Fein, E.D., Hannon, E., Mechanick, J.I. and Benjamin, E. (1996) Transthoracic bioimpedance can measure extravascular lung water in acute lung injury. *Journal of Surgical Research*, **65**, 101-108.

Noble, T.J., Harris, N.D., Morice, A.H., Milnes, P. and Brown, B.H. (2000) Diuretic induced change in lung water assessed by electrical impedance tomography. *Physiological Measurement*, **21**, 155-163.

Noble, T.J., Morice, A.H., Milnes, P., Harris, N.D., Leathard, A.D., Smith, S. and Brown, B.H. (1997) Electrical impedance tomographic spectroscopy in the detection of increased lung water in heart failure. In *Proceedings of the 18th Annual International Conference of the Ieee Engineering in Medicine and Biology Society, Vol 18, Pts 1-5*. I E E E, New York, Vol. 18, pp. 778-779.

Nsah, E., Berger, R.D., Rosenthal, L.S., Hui, R., Ramza, B., Jumrussirikul, P., Lawrence, J.H., Tomaselli, G.F., Kass, D. and Calkins, H. (1998) Initial impedance predicts temperature during radiofrequency catheter ablation. *Journal of the American College of Cardiology*, **31**, 254A-254A.

Olgin, J.E., Kalman, J.M., Chin, M., Stillson, C., Maguire, M., Ursel, P. and Lesh, M.D. (1997) Electrophysiological Effects of Long, Linear Atrial Lesions Placed Under Intracardiac Ultrasound Guidance. *Circulation*, **96**, 2715-2721.

Panescu, D., Webster, J.G. and Stratbucker, R.A. (1994) Modeling Current-Density Distributions During Transcutaneous Cardiac Pacing. *Ieee Transactions on Biomedical Engineering*, **41**, 549-555.

Panescu, D., Whayne, J.G., Fleischman, S.D., Mirotznik, M.S., Swanson, D.K. and Webster, J.G. (1995) 3-Dimensional Finite-Element Analysis of Current-Density and Temperature Distributions During Radiofrequency Ablation. *IEEE Transactions on Biomedical Engineering*, **42**, 879-890.

Patterson, R. (2000) Bioelectric Impedance Measurements. In Bronzino, J.D. (ed.), *The Biomedical Engineering Handbook*. Boca Raton: CRC Press Heidelberg Springer in cooperation by IEEE Press, pp. 73-71 - 73-78.

Petersen, H.H., Chen, X., Pietersen, A., Svendsen, J.H. and Haunso, S. (1999) Temperature-controlled radiofrequency ablation of cardiac tissue: An in vitro study of the impact of electrode orientation, electrode tissue contact pressure and external convective cooling. *Journal of Interventional Cardiac Electrophysiology*, **3**, 257-262.

Pethig, R. (1984) Dielectric-Properties of Biological-Materials - Biophysical and Medical Applications. *Ieee Transactions on Electrical Insulation*, **19**, 453-474.

Petrova, G.I. (1999) Influence of electrode impedance changes on the common-mode rejection ratio in bioimpedance measurements. *Physiological Measurement*, **20**, N11-N19.

Pfitzmann, R., Muller, J., Grauhan, O. and Hetzer, R. (2000) Intramyocardial impedance measurements for diagnosis of acute cardiac allograft rejection. *Annals of Thoracic Surgery*, **70**, 527-532.

Plonsey, R. and Barr, R. (1982) The 4-Electrode Resistivity Technique as Applied to Cardiac-Muscle. *IEEE Transactions on Biomedical Engineering*, **29**, 541-546.

Rabbat, A. (1988) Tissue Resistivity. In Hilger, A. (ed.), *Electrical Impedance Tomography*. Bristol & New York, p. Chap. 2.

Ragheb, T. and Geddes, L.A. (1990) Electrical-Properties of Metallic Electrodes. *Medical & Biological Engineering & Computing*, **28**, 182-186.

Ramos-Castro, J., Bragos, R., García-González, M.A., Salazar, Y., Fontova, A., Bayés-Genis, A., Rosell, J. and Cinca, J. (2003) Sistema de medida multiparamétrico para la detección de rechazo en transplante cardiaco. *Congreso Annual de la Sociedad Española de Ingenieria Biomedica*, Merida, España, pp. 45-48.

Remp, T., Hoffmann, E., Dorwarth, U., Mueller, D., Fiek, M., Gruenewald, A. and Steinbeck, G. (1997) A new catheter design for validation of preablation impedance as a marker for myocardial wall contact before catheter ablation. *Journal of the American College of Cardiology*, **29**, 2168-2168.

Rigaud, B. and Morucci, J.P. (1996) Bioelectrical impedance techniques in medicine .3. Impedance imaging - First section: General concepts and hardware. *Critical Reviews in Biomedical Engineering*, **24**, 467-597.

Rigaud, B., Morucci, J.P. and Chauveau, N. (1996) Bioelectrical impedance techniques in medicine .1. Bioimpedance measurement - Second section: Impedance spectrometry. *Critical Reviews in Biomedical Engineering*, **24**, 257-351.

Riu, P. (1991) Detecciò d'estructures est'atiques en el cos hum'a usant m'etodes multifreqüencia en tomografia d'impedancia elèctrica. *Departament d'enginyeria electrònica*. Universitat Politècnica de Catalunya, Barcelona, España, p. 219.

Riu, P., Rosell, J., Bragos, R. and Casas, O. (eds.). (1999) *Electrical Bioimpedance Methods: applications to medicine and biotechnology*. Annals of the New York Academy of Sciences.

Roberts, D.E., Hersh, L.T. and Scher, A.M. (1979) Influence of Cardiac Fiber Orientation on Wavefront Voltage, Conduction-Velocity and Tissue Resistivity in the Dog. *Circulation Research*, **44**, 701-712.

Roberts, D.E. and Scher, A.M. (1982) Effect of Tissue Anisotropy on Extracellular Potential Fields in Canine Myocardium Insitu. *Circulation Research*, **50**, 342-351.

Rodriguez, E.R. (2003) The pathology of heart transplant biopsy specimens: Revisiting the 1990 ISHLT working formulation. *Journal of Heart and Lung Transplantation*, **22**, 3-15.

Rosell, J., Bragos, R., Casas, O., Warren, M., Tresanchez, M. and Cinca, J. (1999) Bioimpedance Spectroscopy applied to myocardial tissue characterization. *11th Nordic-Baltic Conference on Biomedical Engineering*. Med Biol Eng & Comp, Tallinn, Estonia, Vol. 37(1), pp. 51-53.

Rosell, J., Cohen, K.P. and Webster, J.G. (1995) Reduction of Motion Artifacts Using a 2-Frequency Impedance Plethysmograph and Adaptive Filtering. *IEEE Transactions on Biomedical Engineering*, **42**, 1044-1048.

Rosell, J., Colominas, J., Riu, P., Pallas-Areny, R. and Webster, J.G. (1988) Skin impedance from 1 Hz to 1 MHz. *IEEE Transactions on Biomedical Engineering*, **35**, 649-651.

Rosell, J., Salazar, Y., Ferre, C., Blanco-Enrich, R. and Bragos, R. (2001) Measurement of respiratory related changes using multisine impedance spectroscopy. *11th International Conference on Electrical Bio-Impedance*, Oslo, Norway, pp. 293-296.

Rosell, J. and Webster, J.G. (1995) Signal-to-Motion Artifact Ratio Versus Frequency for Impedance Pneumography. *IEEE Transactions on Biomedical Engineering*, **42**, 321-323.

Rush, S., McFee, R. and Abildskov, J.A. (1963) Resistivity of Body Tissues at Low Frequencies. *Circulation Research*, **12**, 40-&.

Sahakian, A.V., Tompkins, W.J. and Webster, J.G. (1985) Electrode Motion Artifacts in Electrical-Impedance Pneumography. *Ieee Transactions on Biomedical Engineering*, **32**, 448-451.

Schaefer, M., Gross, W., Ackemann, J. and Gebhard, M.M. (2002) The complex dielectric spectrum of heart tissue during ischemia. *Bioelectrochemistry*, **58**, 171-180.

Schafer, M., Schlegel, C., Kirlum, H.-J., Gersing, E. and Gebhard, M.M. (1998) Monitoring of damage to skeletal muscle tissues caused by ischemia. *Bioelectrochemistry and Bioenergetics*, **45**, 151-155.

Scharfetter, H., Hartinger, P., Hinghofer-Szalkay, H. and Hutten, H. (1998) A model of artefacts produced by stray capacitance during whole body or segmental bioimpedance spectroscopy. *Physiological Measurement*, **19**, 247-261.

Schneck, D.J. (2000) An Outline of Cardiovascular Structure and Function. In Bronzino, J.D. (ed.), *The Biomedical Engineering Handbook*. CRC Press in cooperation with IEEE Press, Vol. 1, pp. 1-1:1-12.

Schwan, H.P. (1995) The bioimpedance field: some historical observations. In Gersing, E. and Schaefer, M. (eds.), *IX International Conference on Electrical Bio-Impedance*. ICPRBI, Heidelberg, Germany, Vol. 1, pp. 1-4.

Schwartzman, A., Wolf, T., Gepstein, L., Hayam, G., Lessick, J., Reisfeld, D., Schwartz, Y., Uretzky, G. and Ben-Haim, S.A. (2001) Characterisation of acute myocardial ischaemia in a canine model based on principal component analysis of unipolar endocardial electrograms. *Medical & Biological Engineering & Computing*, **39**, 571-578.

Schwartzman, D., Chang, I., Michele, J.J., Mirotznik, M.S. and Foster, K.R. (1999) Electrical impedance properties of normal and chronically infarcted left ventricular myocardium. *Journal of Interventional Cardiac Electrophysiology*, **3**, 213-224.

Semenov, S.Y., Svenson, R.H., Bulyshev, A.E., Souvorov, A.E., Nazarov, A.G., Sizov, Y.E., Posukh, V.G., Pavlovsky, A.V., Repin, P.N. and Tatsis, G.P. (2000) Spatial resolution of microwave tomography for detection of myocardial ischemia and infarction-experimental study on two-dimensional models. *Ieee Transactions on Microwave Theory and Techniques*, **48**, 538-544.

Smallwood, R.H., Hampshire, A.R., Brown, B.H., Primhak, R.A., Marven, S. and Nopp, P. (1999) A comparison of neonatal and adult lung impedances derived from EIT images. *Physiological Measurement*, **20**, 401-413.

Steendijk, P., Mur, G., Vandervelde, E.T. and Baan, J. (1993) The 4-Electrode Resistivity Technique in Anisotropic Media - Theoretical-Analysis and Application on Myocardial Tissue in-Vivo. *IEEE Transactions on Biomedical Engineering*, **40**, 1138-1148.

Steendijk, P., Vandervelde, E.T. and Baan, J. (1994) Dependence of Anisotropic Myocardial Electrical-Resistivity on Cardiac Phase and Excitation-Frequency. *Basic Research in Cardiology*, **89**, 411-426.

Streeter, D., Jr, Spotnitz, H., Patel, D., Ross, J., Jr and Sonnenblick, E. (1969) Fiber orientation in the canine left ventricle during diastole and systole. *Circulation Research*, **24**, 339-347.

Streeter, D.D. and Hanna, W.T. (1973a) Engineering Mechanics for Successive States in Canine Left Ventricular Myocardium .2. Fiber Angle and Sarcomere Length. *Circulation Research*, **33**, 656-664.

Streeter, D.D. and Hanna, W.T. (1973b) Engineering Mechanics for Successive States in Canine Left-Ventricular Myocardium .1. Cavity and Wall Geometry. *Circulation Research*, **33**, 639-655.

Streeter, D.D., Vaishnav, R.N., Patel, D.J., Spotnitz, H.M., Ross, J. and Sonnenbl.Eh. (1970) Stress Distribution in Canine Left Ventricle During Diastole and Systole. *Biophysical Journal*, **10**, 345-&.

Strickberger, S.A., Vorperian, V.R., Man, K.C., Williamson, B.D., Kalbfleisch, S.J., Hasse, C., Morady, F. and Langberg, J.J. (1994) Relation between Impedance and Endocardial Contact During Radiofrequency Catheter Ablation. *American Heart Journal*, **128**, 226-229.

Trayanova, N.A., Roth, B.J. and Malden, L.J. (1993) The Response of a Spherical Heart to a Uniform Electric-Field - a Bidomain Analysis of Cardiac Stimulation. *Ieee Transactions on Biomedical Engineering*, **40**, 899-908.

Tresanchez, M., Bragos, R., Riu, P.J., Yañez, A., Warren, M., Carreño, A. and Cinca, J. Espectro de la impedancia del miocardio porcino in situ durante la isquemia. Parte II:resultados y modelizacion. *XIV Congreso Anual de la Sociedad Española de Ingeniería Biomédica*, pp. 101-103.

Tsai, J.Z., Cao, H., Tungjitkusolmun, S., Woo, E.J., Vorperian, V.R. and Webster, J.G. (2000) Dependence of apparent resistance of four-electrode probes on insertion depth. *IEEE Transactions on Biomedical Engineering*, **47**, 41-48.

Tsai, J.Z., Will, J.A., Hubbard-Van Stelle, S., Cao, H., Tungjitkusolmun, S., Choy, Y.B., Haemmerich, D., Vorperian, V.R. and Webster, J.G. (2002) In-vivo measurement of swine myocardial resistivity. *IEEE Transactions on Biomedical Engineering*, **49**, 472-483.

Tsai, J.Z., Will, J.A., Vorperian, V.R., Hubbard-Van Stelle, S., Cao, H., Tungjitkusolmun, S., Bin Choy, Y. and Webster, J.G. (2003) In vitro measurement of myocardial impedivity anisotropy with a miniature rectangular tube. *IEEE Transactions on Biomedical Engineering*, **50**, 528-532.

Tungjitkusolmun, S., Woo, E.J., Cao, H., Tsai, J.Z., Vorperian, V.R. and Webster, J.G. (2000) Thermal-electrical finite element modelling for radio frequency cardiac ablation: effects of changes in myocardial properties. *Medical & Biological Engineering & Computing*, **38**, 562-568.

Vivekananthan, K., Kalapura, T., Mehra, M.R., Lavie, C.J., Milani, R.V., Scott, R.L. and Park, M.H. (2002) Usefulness of the combined index of systolic and diastolic myocardial performance to identify cardiac allograft rejection. *The American Journal of Cardiology*, **90**, 517-520.

Wang, Y.Q., Haynor, D.R. and Kim, Y. (2001a) A finite-element study of the effects of electrode position on the measured impedance change in impedance cardiography. *IEEE Transactions on Biomedical Engineering*, **48**, 1390-1401.

Wang, Y.Q., Haynor, D.R. and Kim, Y. (2001b) An investigation of the importance of myocardial anisotropy in finite-element modeling of the heart: Methodology and application to the estimation of defibrillation efficacy. *IEEE Transactions on Biomedical Engineering*, **48**, 1377-1389.

Warren, M., Bragos, R., Casas, O., Rodriguez-Sinovas, A., Rosell, J., Anivarro, I. and Cinca, J. (2000) Percutaneous electrocatheter technique for on-line detection of healed transmural myocardial infarction. *Pace-Pacing and Clinical Electrophysiology*, **23**, 1283-1287.

Warren, M., Casas, O., Bragos, R., Tresanchez, M., Carreño, A., Rodriguez-Sinovas, A., Yañez, A., Rosell, J., Riu, P.J. and Cinca, J. (1998) Timecourse of myocardial tissue electrical impedance during ischemia and reperfusion in in vivo pig hearts. *ICEBI X, International Conference on Electrical Bio Impedance*, Barcelona, Spain, pp. 81-84.

Weller, G.E.R., Lu, E., Csikari, M.M., Klibanov, A.L., Fischer, D., Wagner, W.R. and Villanueva, F.S. (2003) Ultrasound Imaging of Acute Cardiac Transplant Rejection With Microbubbles Targeted to Intercellular Adhesion Molecule-1. *Circulation*, **108**, 218-224.

Williams, P.A. and Saha, S. (1996) The electrical and dielectric properties of human bone tissue and their relationship with density and bone mineral content. *Annals of Biomedical Engineering*, **24**, 222-233.

Wolf, T., Gepstein, L., Hayam, G., Zaretzky, A., Shofty, R., Kirshenbaum, D., Uretzky, G., Oron, U. and Ben-Haim, S.A. (2001) Three-dimensional endocardial impedance mapping: a new approach for myocardial infarction assessment. *American journal of physiology. Heart and circulatory physiology*, **280**, H179-188.

Zanchi, E., Piazza, V., Prati, F., Risa, A.L., Greco, C., Turitto, G. and Prati, P.L. (1995) Transient myocardial ischemia detected by Holter monitoring during the early post/infarction period. *Coronary Artery Disease*, **6**, 389-396.

Zhang, J., Tsai, J.Z., Cao, H., Chen, Y., Will, J.A., Vorperian, V.R. and Webster, J.G. (2003) Noncontact radio-frequency ablation for obtaining deeper lesions. *IEEE Transactions on Biomedical Engineering*, **50**, 218-223.

Zheng, X.S., Walcott, G.P., Hall, J.A., Rollins, D.L., Smith, W.M., Kay, G.N. and Ideker, R.E. (2000) Electrode impedance: An indicator of electrode-tissue contact and lesion dimensions during linear ablation. *Journal of Interventional Cardiac Electrophysiology*, **4**, 645-654.

Artículos en revistas

1. Yolocuauhtli Salazar, Juan Cinca and Javier Rosell **Effect of electrode locations and respiration in the characterization of myocardial tissue using a transcatheter impedance method** *Physiological Measurements* (Aceptado, Mayo 2004).
2. Yolocuauhtli Salazar, Ramon Bragos, Juan Cinca, Javier Rosell **Transmural versus Non-Transmural In situ Electrical Impedance Spectrum for Healthy, Ischemic and Healed Myocardium**. *IEEE Transactions on Biomedical Engineering* (Aceptado Feb 1, 2004).

Congresos Internacionales

1. Yolocuauhtli Salazar, Ramon Bragos, Antonio Bayes-Genis, Juan Cinca, Javier Rosell **Effect of catheter position in transcatheter myocardium electrical impedance measurements** *XII International Conference on Electrical Bio-Impedance* Gdansk, Polonia, vol. I. pp. 107-110. 20-24 June 2004. ISBN: 83-917681-6-3.
2. Ramon Bragós, Juan Ramos, Yolocuauhtli Salazar, Andreu Fontova, Mireya Fernández, Pere Riu, Miguel Ángel García-González, Antoni Bayés-Genís, Juan Cinca and Javier Rosell-Ferrer. **Endocardial impedance spectroscopy system using transcatheter method.** *XII International Conference on Electrical Bio-Impedance* Gdansk, Polonia, vol. II. pp. 465-468. 20-24 June 2004. ISBN:83-917681-6-3.
3. Juan Ramos-Castro, Ramon Bragós-Bardia, Miguel Ángel García-González, Yolocuauhtli Salazar, Andreu Fontova, Antoni Bayés-Genís, Juan Cinca-Cuscullola and Javier Rosell-Ferrer **Multiparametric Measurement System for Detection of Cardiac Graft Rejection** *IMTC 2004 Instrumentation and Measurement Technology Conference* Como, Italy, 18-20 May 2004. vol. 3 pp 1701-05. ISBN: 0-7803-8248-X. ISSN: 1091-5281.
4. Juan Cinca, Yolocuauhtli Salazar, Xavier Viñolas, Juan Ramos, E. Rodríguez Font, Ramon Bragos, Miguel Angel García-González, Antoni Bayés-Genís. **Endocardial temperature and electrical impedance of the normal human heart** Enviado al *Congreso Europeo de Cardiología* 2004.

5. Yolocuauhtli Salazar, Ramon Bragos, Javier Rosell **Transcatheter measurement of myocardium electrical impedance: 2 versus 3 electrode method** *Proc of 25th Annual International Conference of the IEEE Engineering in Medicine and Biology Society* September 17-21, 2003. Cancun, México. pp. 3102-3105. ISBN: 0-7803-7790-7.
6. Yolocuauhtli Salazar, Pere J Riu and Javier Rosell **Effect of Catheter position during intracavitary impedance measurements**. *Proc of World Congress on Medical Physics and Biomedical Engineering* August 24-29, 2003. Sydney, Australia. ISSN: 1727-1983. ISBN: 1-877040-14-2.
7. Yolocuauhtli Salazar, Hermann Scharfetter, Robert Merwa, Antonio Bayés-Genis, Juan Cinca, Ramon Bragós, Javier Rosell **A 3D finite element thorax model for non invasive acute ischemia detection by impedance spectroscopy** *IFMBE Proc 2nd European Medical and Biological Engineering Conference* December 4-8 2002, Wien, Austria. pp. 74-78. ISBN: 3-901351-62-0. ISSN: 1680-0737
8. Javier Rosell, Yolocuauhtli Salazar, Carles Ferre, Ricard Blanco and Ramon Bragós **Measurement of respiratory related changes using multisine impedance spectroscopy** *11th International Conference on Electrical Bio-Impedance ICEBI*, June 17-21, 2001, Oslo. pp. 293-296. ISBN 82-91853-05-3.

Congresos Nacionales

1. Yolocuauhtli Salazar, Ramon Bragós, Juan Ramos, Juan Cinca, y Javier Rosell **Caracterización de tejidos cardiacos mediante métodos invasivos, mínimamente invasivos o no invasivos basados en espectroscopia de impedancia eléctrica**. *IV Jornades de Recerca en Engenyeria Biomèdica*. 8-10 Junio de 2004, Barcelona, España. pp 76-81. ISBN 84-699-8705-4.
2. Juan Ramos Castro, Ramón Bragos Bardia, Miguel Angel García González, Yolocuauhtli Salazar, Andreu Fontova, Antoni Bayes Genis, Javier Rosell Ferrer y Juan Cinca Cuscullola. **Sistema de medida multiparamétrico para la detección de rechazo en transplante cardiaco**. *Proc del Congreso Annual de la Sociedad Española de Ingenieria Biomedica CASEIB 2003* Nov 13-15, 2003. Mérida, España. pp. 45-48. ISBN: 84-688-3819-5. D.L.: SE-3742-03.
3. Miguel Angel García González, Juan Ramos Castro, Yolocuauhtli Salazar, Ramón Bragos Bardia, Antoni Bayes Genís, Javier Rosell Ferrer y Juan Cinca Cuscullola. **Obtención del perfil de temperatura intracardiaco y su variación con la respiración en modelos porcinos anestesiados**. *Proc del Congreso Anual de la Sociedad Española de Ingeniería Biomédica CASEIB 2003* Nov 13-15, 2003. Mérida, España. pp. 187-190. ISBN: 84-688-3819-5. D.L.: SE-3742-03.

4. Yolocuauhtli Salazar, Ramon Bragós, Antonio Bayés-Genis, Hermann Scharfetter, Juan Cinca, Javier Rosell **Detección No Invasiva de Isquemia Aguda por Espectroscopia de Impedancia Eléctrica: Modelo 3D de Elementos Finitos Del Tórax** *Proc XX Congreso Anual de la Sociedad Española de Ingeniería Biomédica CASEIB 2002*. 27-29 de Nov, 2002, Zaragoza, España. pp. 215-218. ISBN: 84-600-9818-4.

5. Yolocuauhtli Salazar, Ramon Bragós, Antonio Bayés, Juan Cinca, Javier Rosell **Evaluación de la Isquemia de Miocardio Mediante Impedancia Eléctrica: Análisis de Modelos 2D y 3D de Elementos Finitos del Tórax** *III Jornades de Recerca en Engenyeria Biomèdica*.13-14 Junio Vic, España. pp 76-81. ISBN 84-699-8705-4.

Si en la lucha el destino te derriba,
si todo en tu camino es cuesta arriba,
si tu sonrisa es ansia insatisfecha,
si hay siembra excesiva y pésima cosecha,
si a tu caudal se le oponen diques,
date una tregua,
pero no claudiques.

-RUDYARD KIPLING-